PHYSICAL REVIEW B, VOLUME 64, 125114

Electron exchange in the *f*-*f* excitations of EuO

B. Fromme, V. Bocatius, and E. Kisker
Institut für Angewandte Physik, Heinrich-Heine-Universität, D-40225 Düsseldorf, Germany

(Received 12 February 2001; published 10 September 2001)

We investigated the dipole-forbidden, multiplicity-changing *f*-*f* excitations of Eu^{3+} ions by spin polarized electron energy-loss spectroscopy, using a polarized primary electron beam as well as polarization analysis of the scattered electrons. This is the only experimental technique to prove electron-exchange excitations directly. The *f*-*f* excitations give rise to a variety of intense sharp structures in the energy-loss range between ≈2 and 6 eV. The energy-loss spectra do not change significantly in the primary-energy range between 20 and 100 eV and it could be proved by spin-resolved scattering-geometry dependent measurements that electron exchange is the only excitation mechanism in this energy range. For higher primary energies, the *f*-*f* excitation peaks begin to vanish, as expected for excitations by electron exchange, but they reappear at the $4d$-$4f$ threshold because of a resonant enhancement, caused by simultaneous $4f$-$4f$ and $4d$-$4f$ excitations.

DOI: 10.1103/PhysRevB.64.125114 PACS number(s): 79.20.Uv, 82.80.Pv

INTRODUCTION

The spectroscopy of rare-earth ions in different host lattices and solutions has a long standing history. In particular the electronic transitions within the partially filled $4f$ shells (*f*-*f* excitations) have been subject of investigations since the discovery of very sharp lines in the spectra of lanthanide compounds—arising from such *f*-*f* excitations—in the beginning of the century.[1] The investigations experienced strong intensification during the last forty years due to the realization of various technical applications: the laser transitions of most solid state lasers are *f*-*f* transitions of rare-earth ions[2] (prominent example: Nd^{3+} in the Nd-YAG laser) and often *f*-*f* transitions or other transitions into $4f$ final states are responsible for the occurrence of luminescence in rare-earth doped phosphors. Such phosphors have a wide range of applications. They are not only used in conventional television screens (an *f*-*f* transition of Eu^{3+} ions in Eu-doped Y_2O_3 or YVO_4 provides the red color at the television screen) but also in fluorescence lamps for color LCD's (Ref. 3) and in devices for medical radiography, where x rays are transformed into visible light for which photographic emulsions are much more sensitive.

Even in compounds, the $4f$ electrons in the partially filled $4f$ shell of the rare-earth ions remain localized at the ion. They are effectively shielded by the filled $5s$ and $5p$ shells, which are higher in energy. Therefore, they are hardly affected by the chemical environment and the crystal-field splitting of the $4f$ states, caused by the interaction of the $4f$ electrons with the surrounding ligand ions in the compound, is very small. It is in the order of several 10 meV only or even less[4–9] and therefore orders of magnitude smaller than the crystal-field splitting of the $3d$ states of transition-metal oxides, which is in the order of 1 eV (for a review see Ref. 10). Thus, the *f*-*f* excitation energies of the free rare-earth ions and the identical ions in different compounds and solutions differ only slightly.

All *f*-*f* excitations are dipole forbidden by the parity selection rule $(\Delta l = \pm 1)$. Nevertheless, they are weakly visible in optical spectra due to the possibility of magnetic dipole transitions and—for rare-earth ions in compounds or solutions—in particular to what is often called "induced" or "forced" electric dipole transitions (for a review see Refs. 7 and 11 and the references therein). The latter have been described by van Vleck initially:[12] an admixture of states of opposite parity (*d* or *g* states in this case) into the *f* states due to lattice vibrations causes small, but non-vanishing dipole-matrix elements. A variety of *f*-*f* transitions are additionally forbidden by the spin selection rule $(\Delta S = 0)$, which remains valid for induced electric dipole transitions—but some of these transitions are also weakly observable in absorption spectra. This is attributed to the fact that in particular the heavy rare earths do not exhibit strict Russell-Saunders coupling. They belong to the intermediate coupling regime, where the quantum numbers of the total orbital angular momentum L and the total spin S of an atom or ion and the corresponding dipole selection rules start to lose their significance, whereas J remains a good quantum number.[11] Therefore, *f*-*f* transitions which are strongly forbidden by the spin selection rule of strict Russell-Saunders coupling—such as the Eu^{3+} laser transition $({}^5D_0 \rightarrow {}^7F_2)$—may become weakly allowed in the case of intermediate coupling, because they do not violate the *J*-selection rules of induced electric dipole transitions ($|\Delta J| \leqslant 6$, but $|\Delta J|$ must be even if $J=0$ for initial or final state).[11] Nevertheless, the optical absorption coefficients or the oscillator strengths, respectively, remain small for all *f*-*f* transitions. They deviate from those of ordinary electric dipole-allowed transitions, as the $4f$-$5d$ excitations for example, by several orders of magnitude.[8,11] Thus, for rare-earth compounds with low $4f$-$5d$ excitation energy, the optical spectra below ≈6 eV photon energy are dominated by the very strong $4f$-$5d$ excitations.[5,8,13,14] This is the case for the Eu^{2+} ions ($[Xe]4f^7$ ground-state configuration) in the rock-salt lattice of EuO, for example. Here, the crystal field, provided by the six O^{2-} ions surrounding each Eu ion octahedrally, splits the $5d$ states into a t_{2g} band with maximum between 1.5 and 2 eV and an e_g band around 5 eV. Similar conditions are found for Eu^{2+} ions in the other europium chalcogenides.[8,14,15] Optical absorption spectra exhibit the strong $4f^7 \rightarrow 4f^6 5d$ excitations only, which superpose the weak *f*-*f* excitations to an extend that these cannot be observed. Only in optical spectra of free Eu^{2+} ions,[16] where the

©2001 The American Physical Society

$4f^7 \rightarrow 4f^6 5d$ transitions require more than ≈4 eV excitation energy,[4,13,16] a few *f-f* excitations have been observed. The situation is completely different for Eu^{3+} ions ($[\mathrm{Xe}]4f^6$ ground-state configuration). Here, the $4f^6 \rightarrow 4f^5 5d$ transitions in solutions as well as compounds need an excitation energy of more than ≈8 eV (Ref. 5 and 13) and a large number of *f-f* excitations has been observed in optical spectra (see, for example, Refs. 4, 7, 9, 11, 13, 17, and 18, and references therein).

In contrast to optical absorption measurements, the dipole forbidden *f-f* excitations of rare earths and their compounds are known to be excellently observable in low-energy electron energy-loss spectra. They remain clearly visible in energy-loss spectra obtained with primary-electron energies of up to 100–200 eV and vanish if higher energies are used.[19–24] According to this observation it is suggested, but has not been proved unambiguously up to now (see below), that electron exchange is the relevant excitation mechanism here, because of the primary-energy dependence of exchange processes: electron exchange is usually found to be significant for low primary energies only, which are not substantially larger than the excitation energies (typically ten times). The idea behind this assumption is that exchange becomes more probable when the velocities of the colliding free incident and the bound target electrons become comparable.[25] Whereas electron exchange in excitations of free atoms is in fact often found to be negligible when the incident-electron energy exceeds the excitation energy only slightly,[26] this can be completely different for excitations between atomic-like states in solids: recent spin-polarized electron energy-loss measurements[27–34] as well as theoretical investigations[35] of the excitations between the crystal-field split, localized $3d$ states of the transition-metal oxides NiO, CoO, and MnO clearly show the significance of electron exchange up to primary energies of more than 100 eV. For the *f-f* excitations of Gd also nonvanishing exchange-scattering cross sections have been calculated for incident energies of 100–300 eV.[36,37]

A considerable high amount of electrons, inelastically scattered with energy losses corresponding to the *f-f* excitation energies, is found under large scattering angles—far off specular scattering geometry.[20–23] This is a further hint for the significance of electron-exchange processes in the excitation of *f-f* transitions due to the different angular distribution of electrons, inelastically scattered by different scattering mechanisms (as exchange and dipole scattering for example) as briefly described in the following.

In inelastic electron scattering or excitation by electron impact, respectively, it is customary to distinguish between different scattering mechanisms due to their different theoretical description: ‘‘dipole scattering’’ is describable in the framework of classical dielectric dipole theory.[38–40] The excitation of the target and the scattering of the exciting electron occurs due to the interaction of the electrons' electric field with the target charges. The scattering cross section mainly depends on the dielectric function. A detailed microscopic knowledge of the interaction of incident electron and target is not needed. Excitation by dipole scattering is possible for electric dipole allowed transitions only. It is not accompanied by electron exchange because the excitation is caused by long-range electric fields; excitation and scattering process occur far above the target surface, the incident electron does not penetrate the surface. The angular distribution of the scattered electrons is very small and the scattered electrons are confined to the so-called characteristic ‘‘dipolar lobe’’ around forward direction in high-energy transmission EELS (zero scattering angle), provided energy loss and momentum transfer are small. In the case of low-energy reflection EELS, the dipole-scattered electrons are found in a small dipolar lobe around specular scattering geometry. It is assumed that an elastic scattering process, which follows or precedes the inelastic small-angle dipole scattering, is responsible for the specular reflection of the electrons.

Other scattering mechanisms are usually summarized to what is called ‘‘impact scattering.’’ The denotation impact scattering is not defined precisely and covers nearly all scattering events, not describable by classical dielectric dipole theory as exchange scattering for example. At present, impact scattering is only poorly described by theories, due to the necessity of ‘‘microscopic’’ models, requiring a detailed knowledge of the electron-target interactions, leading to the observed scattering process. Impact or exchange scattered electrons are usually not confined to a small angular range. Their distribution can be angularly wide spread[29,32,34,38,41] or can show a complicated scattering-angle dependence, which depends on the kind of the excited transition.[42–44]

Up to now, the existence of electron exchange in the *f-f* transitions of rare-earth atoms or ions has only indirectly been concluded from the primary-energy and angular dependence of the *f-f* excitation assigned energy-loss structures to our knowledge—it has not directly been proved. The reason for this lack is found in experimental difficulties: for a direct proof of electron-exchange processes, it is necessary to distinguish between inelastically scattered primary electrons and emitted ‘‘true’’ target electrons. But electrons are distinguishable via their spin only. Thus, an unambiguous proof of electron exchange requires both, a polarized primary electron beam and polarization analysis of the scattered electrons and is possible with that kind of spin-polarized electron energy-loss spectroscopy (SPEELS), where a polarized primary electron beam is scattered at the target and energy distribution and polarization of the scattered electrons are measured simultaneously. Apart from the spin-integrated intensity I, which is also measured in EELS with unpolarized electrons, the spin-flip intensity F and the nonflip intensity N can be calculated from the spin-integrated intensity and the polarization of incident electrons P_0 and scattered electrons, P_S: $F = 0.5(1 - P_S/P_0)I$ and $N = 0.5(1 + P_S/P_0)I$.[45] If the polarization of the scattered electron beam deviates from that of the incident one, the spin-flip intensity is not zero and spin-flip exchange processes participate in the investigated transitions. Excitation processes, where the incident electron has been exchanged with a target electron of the same spin direction (nonflip process) cannot be distinguished from direct scattering processes–such as dipole scattering—where incoming and scattered electron are identical.

We now investigated the *f-f* excitations of Eu^{3+} ions in europiumoxide with SPEELS. This seems to be astonishing at first sight, because our samples were nominally stoichiometric EuO(100) single crystals and are therefore expected to contain Eu^{2+}. But our measurements, obtained with low-energy electrons and therefore probing the outer layers of a sample only due to the small penetration depth of such electrons,[46] clearly show the prevalence of Eu^{3+} ions in the EuO surface, thereby proving an earlier assumption about the EuO(100) surface.[47] This is discussed below together with our results.

EXPERIMENTAL SETUP AND SAMPLE PREPARATION

The setup of our SPEELS experiment has been described elsewhere in detail[34,48] and may be summarized here briefly. For the generation of polarized electrons, we use a conventional GaAs source.[49] The initially longitudinally polarized electrons are electrostatically deflected by a 90° spherical deflector to separate the electron beam from the exciting laser beam. The electrons travel through a 180° spherical monochromator and impinge, now transversely polarized, onto the target. The energy distribution of the scattered electrons is measured by use of a 180° spherical analyzer; the polarization is investigated with a high-energy (100 keV) Mott detector. The polarization of the incident electrons P_0 can be measured by applying a repulsive electrostatic potential to the target in such a way that the electrons can reach the Mott detector without interaction with the target. In the measurements reported below $P_0 = 20-25\,\%$. The energy resolution (measured as FWHM of the elastically scattered electrons) is 200–250 meV for primary energies less than $\sim$100 eV. For primary energies up to 200 eV it is slightly higher (up to $\sim$350 meV). In our experimental setup, the scattering angle is determined by the axes of the electron optics and therefore fixed to 90° (incident angle $\theta_i = 45°$, detection angle $\theta_d = 45°$). Scattering-geometry depending measurements are possible by simply rotating the target, which alters incident and detection angle likewise.

The samples, cleaved EuO(100) single crystals, have been grown by a solution sintering process.[50] After insertion into the UHV chamber (base pressure $< 2 \times 10^{-8}$ Pa), the crystals have been sputtered with 500 eV argon ions for several hours. During sputtering and during the SPEELS measurements, the sample temperature was hold at 200–250 °C to avoid charging of the usually insulating samples. With this moderate heating, the electric conductivity is high enough to allow for SPEELS measurements down to $\sim$20 eV primary energy. The surface of the samples was found to change rapidly in particular under electron impact. The Eu^{3+} *f*-*f* transitions where observable at best (with very low "background" intensity arising from other excitations) from several hours up to two days after sputtering. Therefore, the samples had to be sputtered for 0.5–1 h every two days. Consequently, the time for measurements with really identical surface was short. But the spectra, obtained after different sputtering processes were found to differ only slightly.

RESULTS AND DISCUSSION

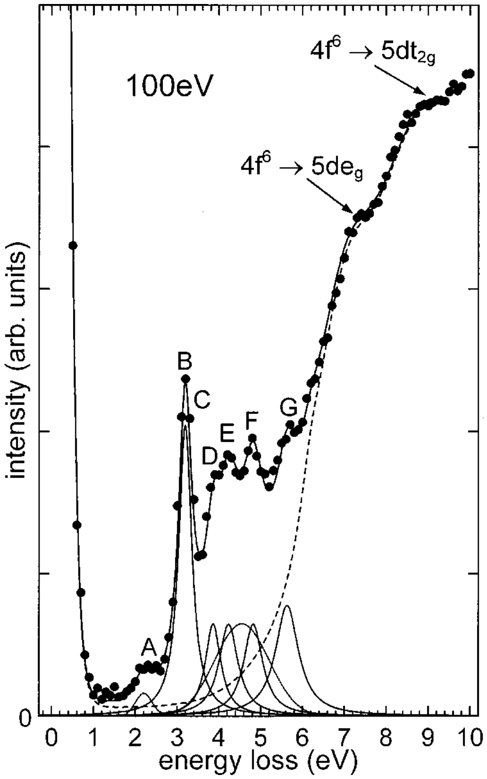

FIG. 1. Energy-loss spectrum, measured with 100 eV primary energy in specular scattering geometry. The energy-loss peaks arising from *f*-*f* excitations of Eu^{3+} ions are denoted by capital letters. The *f*-*f* excitation peaks have been fitted by the Lorentz profiles in the lower part of the figure; the strongly increasing intensity above 5–6 eV, which is assigned to the onset of the dipole-allowed $4f^6 \rightarrow 5d$ excitation of the Eu^{3+} ions, has been fitted by the flank of two Gauss profiles (dashed line). The solid line through the data points is the addition of these profiles and the two Gauss profiles at 2.2 and 4.5 eV (dotted lines), which may indicate the $4f^7 \rightarrow 5dt_{2g}$ and $4f^7 \rightarrow 5de_g$ excitations of some still present Eu^{2+} ions.

A spin-integrated energy-loss spectrum, measured with 100 eV primary energy in specular scattering geometry ($\theta_i = \theta_d = 45°$), is shown in Fig. 1. In the low-energy part (<6 eV energy loss) the spectrum is dominated by relatively sharp energy-loss peaks ($A-G$). Nearly all these energy-loss peaks can unambiguously be assigned to the superposition of a variety of close lying, atomiclike, multiplicity-changing *f*-*f* excitations $[{}^7F \rightarrow {}^5X,\ {}^3Y\ (X = D,L,G,H,F,I,\ldots;\ Y = P,I,\ldots)]$ of Eu^{3+} ions. The measured excitation energies are listed in Table I. In the limits of energy resolution, they are in accordance with calculations[7] and results of optical measurements at free Eu^{3+} ions[4] as well as Eu^{3+} ions in solids and solutions.[9,17,18] Only the relatively weak structure D (3.9 eV energy loss) may contain contributions of *f*-*f* excitation of Eu^{2+} ions: the ${}^8S \rightarrow {}^6I$ transition of the $4f^7$ configuration requires such an excitation energy.[16,19] Transitions form the ${}^7F_0$ ground state of Eu^{3+} into final states with odd quantum number J (Table I) are not observed in optical absorption spectra. For excitation by photons, such final states can be reached only from the excited fine-structure levels (${}^7F_1$, ${}^7F_2,\ldots$) due to the selection rules for J (see above). This must not be true for excitations with electrons. However, because of the sample temperature of 200–250 °C in

TABLE I. Energies of the *f-f* excitation assigned energy-loss peaks (this work) in comparison with results obtained by optical spectroscopy and calculations for free Eu^{3+} and Eu^{3+} ions in different host crystals and solutions (Refs. 5, 8, 10, 18, and 19). Each energy-loss peak measured by us, contains contributions of a variety of close trying *f-f* excitations from $^7F_0$ and $^7F_1$ initial states into different $4f$ final states. The capital letters correspond to the notation of Fig. 1.

	Measured and calculated $4f$ excitation energies of Eu^{3+} in different surroundings (eV)		
Peaks	SPEELS (this work)	Optical spectroscopy and calculations	$4f$ final states of Eu^{3+}
A	~2–3	2.1–3.03	^5D_J $(J=0-3)$
B	3.2	3.1–3.5	^5L_J $(J=6-10)$
C	3.4		$^5D_4$ ^5G_J $(J=2-6)$
D	3.9	3.8–4.0	^5H_J $(J=3-7)$
E	4.2 4.4(?)	4.1–4.6	^5F_J $(J=1-5)$ ^5I_J $(J=4-8)$ ^5K_J $(J=5,6)$ $^3P_0$
F	4.8	4.7–4.95	^5K_J $(J=7-9)$ ^5G_J $(J=2-4)$ $^3K_6$ $^3I_6$ $^3P_1$
G	5.6		

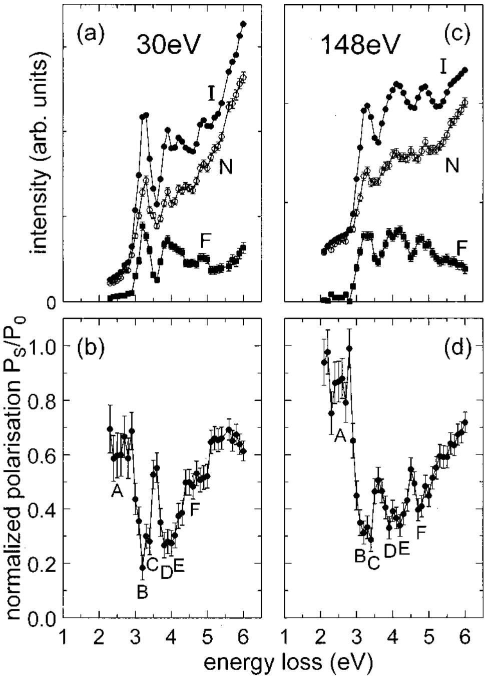

FIG. 2. Spin-resolved energy-loss spectra, measured in specular scattering geometry with 30 and 148 eV primary energy. (a),(c) Spin-integrated intensity *I* (●), Nonflip intensity *N* (○), and spin-flip intensity *F* (■). (b),(d) Polarization of the scattered electrons, normalized to the polarization of the incident ones. The capital letters in (b) and (d) correspond to the notation of Fig. 1 and Table I.

the measurements, the $^7F_0$ ground state and the first excited fine-structure level ($^7F_1$), lying around 45 meV higher in energy, exhibit nearly identical occupation numbers and also the $^7F_2$ level (~126 meV) is occupied to a small amount. Therefore, in the limits of energy resolution, excitations from all these levels must be expected to contribute to the *f-f* excitation assigned energy-loss peaks. The *f-f* excitations within the spin-orbit split ^7F_J ground-state multiplet ($J=0...6$), which require excitation energies of ~45–600 meV, have been investigated by us with high-resolution electron energy-loss spectroscopy (HREELS) recently. These results will be published elsewhere.

Spin-resolved electron energy-loss spectra, obtained with 30 and 148 eV primary energy, are shown in Fig. 2. Because of the very low counting rates in spin-resolved measurements,[34] the data-acquisition time is very long. For each spectrum of Fig. 2 it was more than 40 h. Therefore, such spin-resolved measurements have been done for selected primary energies only. The spin-resolved spectra clearly show that the *f-f* excitations are excited by electron exchange: in the *f-f* excitation assigned energy-loss peaks, the polarization of the scattered electrons deviates more or less strongly from that of the incoming ones; the *f-f* excitations appear as distinct minima in the polarization curves [$A-F$ in Figs. 2(b), 2(d)]. Due to the high change in polarization in the scattering process, all *f-f* excitations appear in the spin-flip intensity [F in Figs. 2(a) and 2(c)] indicating a high amount of spin-flip exchange transitions. Peak *C*, which is strongly superposed by peak *B* and therefore invisible in spin-integrated measurements (Fig. 1), is clearly visible in the spin-resolved spectra (Fig. 2), due to its strong appearance in the spin-flip spectrum and in the polarization curve.

The broad energy-loss structure around 2–2.7 eV (*A* in Figs. 1 and 2) is probably due to a variety of near lying $^7F_0$, $^7F_1 \rightarrow {}^5D_J$ $(J=0-3)$ excitations (Table I). But it may also be assigned to the $4f^7 \rightarrow 5dt_{2g}$ transitions of Eu^{2+} ions, provided some divalent ions are still existing in or near the surface. The excitation energy is nearly identical to that of the $4f^7 \rightarrow 5dt_{2g}$ transitions of Eu^{2+} ions in the mixed valency compound Eu_3O_4,[5] which contains Eu^{2+} ions and Eu^{3+} ions in the ratio 1:2. The $4f^7 \rightarrow 5de_g$ transitions of some remaining Eu^{2+} ions may give rise to the broadly distributed intensity under the *f-f* excitation peaks $D-F$: in fact, our energy-loss spectra can excellently be fitted only (solid line through the data points of Fig. 1), if a broadly distributed intensity between 3.5 and 5.5 eV (dotted Gauss profile in Fig. 1) is added to the Lorentz profiles of the *f-f* excitations (solid lines in the lower part of Fig. 1). A lot of $4f^7 \rightarrow 5d$ transitions are dipole allowed. Therefore, it can be expected that they are strongly excited by the dipole-scattering mechanism and mainly appear in the nonflip channel of the spin-resolved spectra. This is the case, indeed, as our spin-resolved spectra (Fig. 2) show: the weak energy-loss structure A mainly appears in the nonflip intensity (the polarization deviates only slightly from that of the incident electrons) and also in the energy range between ~3.5 and 5 eV energy loss, where we suppose the $4f^7 \rightarrow 5de_g$ transitions, the spectra exhibit a more or less flat, relatively high nonflip intensity. The *f*-*f* excitations in this energy range $(D-F)$, which are excited by electron exchange and therefore found in flip and nonflip intensity, are superposed onto this intensity. Considering the energy difference between $4f^7 \rightarrow 5dt_{2g}$ and $4f^7 \rightarrow 5de_g$ excitations, a crystal-field splitting of the $5d$ states of the order of ~2 eV can be concluded. We assign the broad structures around 7 and 9 eV (Fig. 1) to the $4f^6 \rightarrow 5dt_{2g}, 5de_g$ excitations of the trivalent ions—here also the crystal-field splitting of 2 eV appears. In addition, apart from the *f*-*f* excitations, which are expected to appear in optical spectra with very low intensity only (see above), the energy-loss spectrum looks very similar to the imaginary part of the dielectric function of Eu_3O_4—obtained from optical reflectivity measurements[5]—but with a slightly higher crystal-field splitting of the $5d$ states (~2 eV here, ~1.3 eV in Eu_3O_4).

Our EuO samples did not show any LEED patterns, indicating a disordered surface. Disorder and deviation from stoichiometry has been observed for EuO(100) surfaces previously and assigned to the existence of trivalent Eu ions in the surface: Felton *et al.*[47] reported stable, but initially disordered EuO(100) surfaces, which showed no LEED patterns. (In contrast, Bas *et al.*[51] observed LEED patterns. But these were time dependent, indicating an unstable surface. The observed differences were attributed to the possibility that the stoichiometry and structure of EuO samples may vary from sample to sample, depending upon the conditions during crystal growth.[47]) Surface sensitive electron energy-loss spectroscopic measurements[52] as well as theoretical studies[53] of the rare-earth chalcogenide SmS clearly showed the coexistence of trivalent and divalent Sm ions at the surface. Owing to this results and the observation that neither a pressure burst of oxygen nor a decay of the oxygen Auger signal was observed under electron impact, Felton *et al.*[47] concluded that the disorder of the EuO(100) surface was not associated with electron-stimulated oxygen desorption, but with the formation of trivalent ions at the surface similar as in SmS. That this early suggestion was right is evident by our electron energy-loss results now, which clearly show not only the existence but the prevalence of Eu^{3+} ions near the EuO(100) surface.

Spin-resolved, scattering-geometry dependent measurements of the very intense, dominant structure at 3.2 eV energy loss (peak *B* in Figs. 1, 2 and Table I) are shown in Fig. 3 for different primary energies. Spin-integrated intensity, spin-flip, and nonflip intensity are found to be broadly distributed around specular scattering geometry. They decrease in proportion and nearly symmetrically towards off-specular scattering geometries. The polarization is constant due to the constant ratio of spin-flip and nonflip intensity. An identical scattering-geometry dependence has been observed for the excitations between the localized, crystal-field split $3d$ states of the Mn^{2+} ions in MnO previously (Fig. 4(a); see also Refs. 32 and 34). MnO has a half filled $3d$ shell and all *d*-*d* excitations are—similar to the case of the *f*-*f* excitations of the Eu^{3+} ions investigated here—multiplicity changing. Both, the multiplicity-changing *f*-*f* transitions as well as the multiplicity-changing *d*-*d* transitions are obviously exclusively excited by electron-exchange processes, which often lead to an angularly wide distribution of the scattered electrons (see above). The incoming electrons are exchanged by electrons with opposite and identical spin direction and the scattered electron are therefore found in the spin-flip as well as in the nonflip intensity. Hints for excitations by the dipole scattering mechanism, which are possible for dipole-allowed transitions, are not found. Indicative for such excitations is a high intensity of electrons, scattered into a small angular range around specular scattering geometry, the so-called dipolar lobe, which is found in the nonflip intensity only. In the multiplicity-conserving *d*-*d* transitions of the transition-metal ions in NiO and CoO, which are forbidden by the parity-selection rule only, this nonflip dipolar lobe is in fact ob-

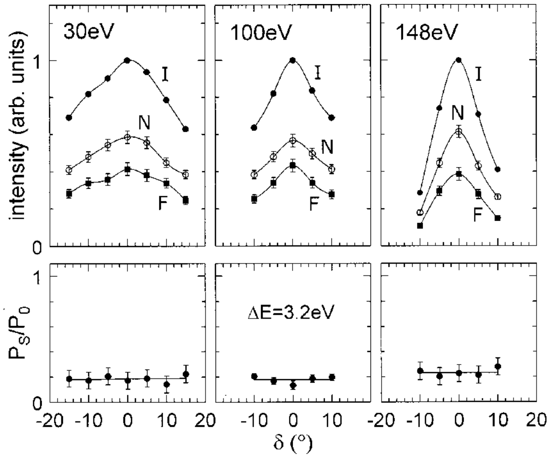

FIG. 3. Scattering-geometry dependence of spin-integrated intensity *I* (●), nonflip intensity *N* (○), and spin-flip intensity *F* (■) at 3.2 eV energy loss for 30, 100, and 148 eV primary energy. The corresponding scattering-geometry dependence of the normalized polarization is plotted in the lower part of the figure. δ is the rotation angle of the sample, $\theta_i = 45° + \delta$, $\theta_d = 45° - \delta$.

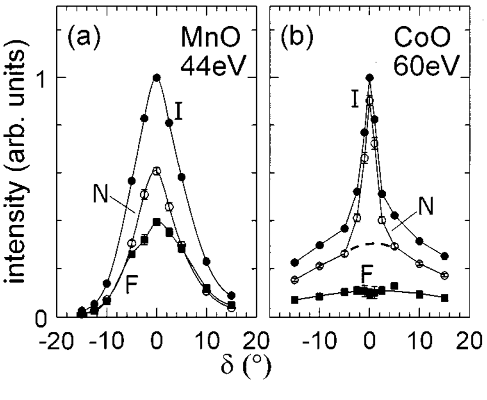

FIG. 4. Scattering-geometry dependence of spin-integrated intensity *I* (●), nonflip intensity *N* (○), and spin-flip intensity *F* (■) of (a) MnO, multiplicity-changing *d*-*d* excitation ($^6A_{1g} \rightarrow {}^4A_{1g}$, ^4E_g with 2.82 eV excitation energy); 44 eV primary energy. (b) CoO, multiplicity-conserving *d*-*d* excitation ($^4T_{1g} \rightarrow {}^4A_{2g}$ with 2 eV excitation energy); 60 eV primary energy. δ is the rotation angle of the sample, $\theta_i = 45° + \delta$, $\theta_d = 45° - \delta$.

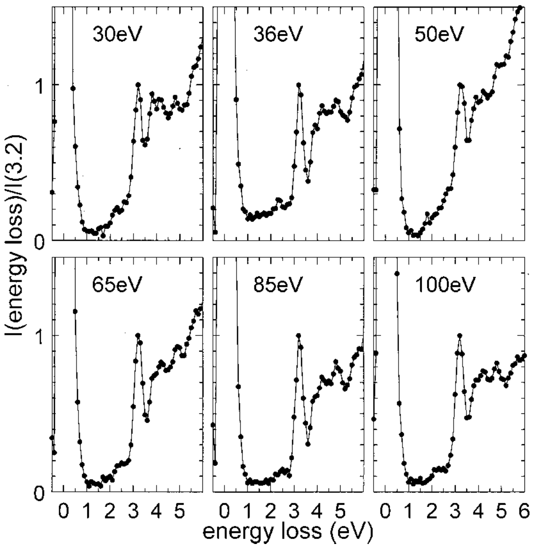

FIG. 5. Spin-integrated energy-loss spectra, measured with different primary energies in specular scattering geometry. The spectra are normalized to the intensity of the 3.2 eV energy-loss peak.

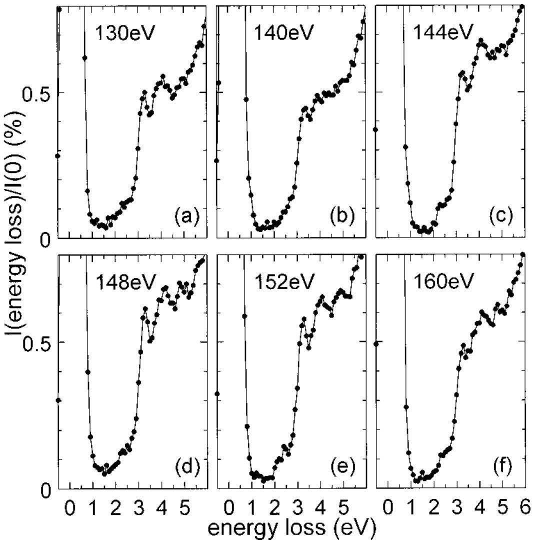

FIG. 6. Spin-integrated energy-loss spectra, measured with different primary energies of more than 130 eV in specular scattering geometry. The spectra are normalized to the intensity of the elastically scattered electrons.

served. It superposes the broadly distributed spin-flip and nonflip intensity, arising from exchange processes, strongly [Fig. 4(b) for CoO and Refs. 27, 32, and 34]. The multiplicity-conserving *d-d* transitions in NiO and CoO become slightly allowed by an admixture of odd parity states into the *d* states in the oxide crystals due to the van Vleck mechanism.[12] The total lack of dipole scattering processes, which can be inferred from our spin-resolved scattering-geometry dependent measurements here, might be a hint that the spin-selection rule remains valid for europium ions (with more or less intermediate coupling of the angular momenta) to an extent, similar to that in the $3d$ transition-metal ions with strict Russell-Saunders coupling.

Spin-integrated energy-loss spectra, measured with different primary energies in specular scattering geometry, are shown in Fig. 5. As can be inferred, the general shape of the energy-loss spectra does not change significantly in this primary-energy range; all *f-f* excitations are clearly visible. The spectra of Fig. 5 have been obtained at different days, after different sputtering processes. Slight differences in the intensity ratios of different energy-loss structures at different primary energies, in particular in the ratio of *f-f* excitation assigned peaks to the background, arising from other transitions as $4f\rightarrow 5d$, for example, must mainly be attributed to slight differences of the surface properties after different sputter processes. The intensity is normalized to the intensity of the dominant energy-loss peak at 3.2 eV in Fig. 5 and not to the intensity of the elastically scattered electrons as often done. Normalization to the intensity of elastically scattered electrons has been found to make sense only for spectra, measured after one sputtering process, because the intensity ratio of inelastically to elastically scattered electrons was found to vary with the surface preparation.

If the primary energy is further increased (Fig. 6), the *f-f* excitation assigned peaks decrease as expected for excitation by electron exchange. At 140 eV primary energy [Fig. 6(b)] the 3.2 eV energy loss (peak *B*) only remains clearly visible. The other ones can hardly be resolved from the broadly distributed intensity at 3.5–5.5 eV, which we attribute to the $4f^7\rightarrow 5de_g$ excitations of remaining Eu^{2+} ions. For primary energies in excess of 140 eV, the *f-f* excitations reappear [Figs. 6(c)–6(e)] but finally decrease with further increasing primary energy [Fig. 6(f)]. This intensity enhancement between ~142 and 156 eV is attributed to a resonant behavior of the *f-f* transitions if the primary energy coincides with the $4d$-$4f$ excitation energy. Such resonance processes are well known phenomena in photoemission spectroscopy as well as electron scattering, when the energy of the incident particle is swept through an inner excitation threshold of the target. In both spectroscopic methods, the resonances are caused by the interference of two excitation channels leading to the same final state, the ''normal'' excitation process, possible at any energy of the incident particle, and the excitation via formation and decay of a temporarily formed resonance compound state, possible at the resonance primary energy only. At the $4d$-$4f$ threshold of the Eu^{3+} ions, the normal *f-f* excitation $4d^{10}4f^6+e^-\rightarrow 4d^{10}4f^{6*}+e^-$ interferes with the $4d^{10}4f^6+e^-\rightarrow 4d^9 4f^8\rightarrow 4d^{10}4f^{6*}+e^-$ excitation, where the incident electron looses its energy in a $4d$-$4f$ excitation. Itself is temporarily captured into a $4f$ state and a $4d^9 4f^8$ resonance compound state is formed. This state can decay by an Auger process, where the six $4f$ electrons of the Eu^{3+} ion remain in an excited state and an electron with energy loss, corresponding to the *f-f* excitation energy, is emitted. The resonance primary-energy range measured by us (~142–156 eV) coincides exactly with the $4d$-$4f$ excitation energy: in electron energy-loss measurements, obtained with high-energy electrons (1760 eV primary energy) at oxidized europium surfaces,[54] the most intense $4d$-$4f$ excitations give rise to a twofold, broad energy-loss structure between ~140–155 eV.

Such resonances at the $4d$-$4f$ threshold have been observed for the *f-f* excitations of a variety of pure rare-earth metals previously.[20–23] Also the excitations between the crystal-field split $3d$ states of the $3d$ transition-metal oxides NiO, CoO, and MnO exhibit a similar weak resonance effect. This occurs at the $3s$-$3d$ threshold.[55,28–34] In these materials, in addition, a much stronger resonance at lower primary energy (36–38 eV) is observed.[28–34] This resonance is attributed to simultaneous *d*-*d* and $O2p$-$O3p$ excitations and requires the possibility of interatomic Auger processes involving oxygen as well as metal ions. For the Eu^{3+} *f*-*f* excitations in europiumoxide measured here, no further resonances have been found in the investigated primary energy range between 20 and 200 eV. Resonances owing to simultaneous excitations involving oxygen states must be excluded. This is a clear hint that the occurrence of interatomic Auger processes is bound to the existence of hybridization between the participating oxygen and metal states: whereas the $O2p$ and metal $3d$ states of the transition-metal oxides are strongly hybridized, the $4f$ electrons of the rare earths are hardly affected by the chemical environment in compounds and retain nearly pure *f* character; a considerable hybridization with states of surrounding oxygen ions can be excluded.

SUMMARY

The earlier proposed significance of electron exchange in the *f*-*f* excitations of rare earths has been proved here for Eu^{3+} ions in europiumoxide using spin-polarized electron energy-loss spectroscopy. Similar as in the case of the *d*-*d* excitations in transition-metal oxides and in accordance with theoretical investigations, electron exchange is found to be the relevant excitation mechanism up to relatively high primary energies, which exceed the excitation energies by more than an order of magnitude. Spin-resolved measurements with variation of the scattering geometry show that the exchange-scattered electrons are angularly wide spread. A sharply around specular scattering geometry peaked nonflip intensity, which is typical for electrons, scattered by a process describable in terms of dielectric dipole theory, is not found. Owing to the fact that excitations accompanied by a dipole scattering process are possible for dipole- or weakly dipole-allowed transitions only, this is a clear hint that the spin-selection rule of strict Russell-Saunders coupling is hardly weakened in the relatively heavy Eu ions.

The *f*-*f* excitations are found to show resonant behavior if the primary energy coincides with the $4d$-$4f$ excitation threshold. Similar resonances have been observed in electron energy-loss investigations of the *f*-*f* excitations of a variety of rare earths and *d*-*d* excitations of several $3d$ transition-metal oxides, previously. In the primary-energy range of 20–200 eV investigated here, the resonance at the $4d$-$4f$ threshold is the only one observed. Further resonances, as such owing to simultaneous excitations involving oxygen states, which have been found to be strong in the case of the *d*-*d* excitations of transition-metal oxides, must be excluded. This is attributed to the missing hybridization between rare earth and oxygen ions in rare-earth compounds.

ACKNOWLEDGMENTS

We are very much indebted to K. J. Fischer for donating the EuO crystals and a lot of valuable discussions. Also the discussions with A. Bringer and W. Urland were very helpful—thank you very much. This work was supported by the Deutsche Forschungsgemeinschaft.

---

[1] J. Becquerel, Phys. Z. **8**, 632 (1908).
[2] Alexander A. Kaminskii, *Laser Crystals* (Springer-Verlag, Berlin, 1981).
[3] T. Fukuzawa, T. Toyooka, Y. Sakaguchi, K. Takeda, and F. Yamada, SID SYM **29**, 247 (1998).
[4] G. H. Dieke and H. M. Crosswhite, Appl. Opt. **2**, 675 (1963).
[5] B. Batlogg, E. Kaldis, A. Schlegel, and P. Wachter, Phys. Rev. B **12**, 3940 (1975).
[6] S. Hüfner, *Optical Spectra of Transparent Rare Earth Compounds* (Academic, New York, 1978).
[7] C. Görller-Walrand and K. Binnemans, in *Handbook on the Physics and Chemistry of Rare Earths* edited by K. A. Gschneidner, Jr. and L. Eyring (Elsevier, Amsterdam, 1996), Vol. 23, p. 121ff.
[8] P. Wachter, CRC Crit. Rev. Solid State Sci. 189ff (1972).
[9] N. C. Chang and J. B. Gruber, J. Chem. Phys. **41**, 3227 (1964).
[10] P. A. Cox, *Transition Metal Oxides* (University Press, Oxford, 1992).
[11] C. Görller-Walrand and K. Binnemans, in *Handbook on the Physics and Chemistry of Rare Earths* edited by K. A. Gschneidner, Jr. and L. Eyring (Elsevier, Amsterdam, 1998), Vol. 25, p. 101ff.
[12] J. H. van Vleck, J. Phys. Chem. **41**, 67 (1937).
[13] W. T. Carnall, in *Handbook on the Physics and Chemistry of Rare Earths*, edited by K. A. Gschneidner, Jr. and L. Eyring (North-Holland, Amsterdam, 1979), p. 171ff.
[14] G. Güntherodt, P. Wachter, and D. M. Imboden, Phys. Kondens. Mater. **12**, 292 (1971).
[15] P. Wachter, in *Handbook on the Physics and Chemistry of Rare Earths*, edited by K. A. Gschneidner, Jr. and L. Eyring (North-Holland, Amsterdam, 1979), p. 507ff.
[16] J. Sugar and N. Spector, J. Opt. Soc. Am. **64**, 1484 (1974).
[17] W. T. Carnall, P. R. Fields, and K. Rajnak, J. Chem. Phys. **49**, 4450 (1968).
[18] L. G. DeShazer and G. H. Dieke, J. Chem. Phys. **38**, 2190 (1963).
[19] E. Bauer and J. Kolaczkiewicz, Phys. Status Solidi B **131**, 699 (1985).
[20] S. Modesti, G. Paolucci, and E. Tosatti, Phys. Rev. Lett. **55**, 2995 (1985).
[21] S. Modesti, F. Della Valle, and G. Paolucci, Phys. Scr. **T19**, 419 (1987).
[22] F. Della Valle and S. Modesti, Phys. Rev. B **40**, 933 (1989).
[23] J. A. D. Matthew, W. A. Henle, M. G. Ramsey, and F. P. Netzer, Phys. Rev. B **43**, 4897 (1991).
[24] A. Gorschlüter, R. Stiller, and H. Merz, Surf. Sci. **252/252**, 272 (1991).

[25] G. F. Hanne, Phys. Rep. **95**, 95 (1983).

[26] Joachim Kessler, *Polarized Electrons* (Springer-Verlag, Berlin, 1985), and references therein.

[27] B. Fromme, M. Schmitt, E. Kisker, A. Gorschlüter, and H. Merz, Phys. Rev. B **50**, 1874 (1994).

[28] B. Fromme, A. Hylla, C. Koch, E. Kisker, A. Gorschlüter, and H. Merz, J. Magn. Magn. Mater. **148**, 181 (1995).

[29] B. Fromme, Ch. Koch, R. Deussen, and E. Kisker, Phys. Rev. Lett. **75**, 693 (1995).

[30] B. Fromme, M. Möller, Th. Anschütz, C. Bethke, and E. Kisker, Phys. Rev. Lett. **77**, 1548 (1996).

[31] B. Fromme, C. Bethke, M. Möller, Th. Anschütz, and E. Kisker, Vacuum **48**, 225 (1997).

[32] B. Fromme, M. Möller, C. Bethke, U. Brunokowski, and E. Kisker, Phys. Rev. B **57**, 12 069 (1998).

[33] B. Fromme, U. Brunokowski, and E. Kisker, Phys. Rev. B **58**, 9783 (1998).

[34] B. Fromme, *d-d Excitations in Transition Metal Oxides—A Spin-Polarized Electron Energy-loss Spectroscopy (SPEELS) Study*, Springer Tracts in Modern Physics Vol. 170 (Springer-Verlag, Berlin, 2000).

[35] J. J. M. Michiels, J. E. Inglesfield, C. J. Noble, V. M. Burke, and P. G. Burke, Phys. Rev. Lett. **78**, 2851 (1997).

[36] S. J. Porter, J. A. D. Matthew, and R. J. Leggott, Phys. Rev. B **50**, 2638 (1994).

[37] H. Ogasawara and A. Kotani, Tech. Rep. ISSP, Ser. A **3050**, 1 (1995).

[38] H. Ibach and D. L. Mills, *Electron Energy Loss Spectroscopy and Surface Vibrations* (Academic Press, New York, 1982).

[39] H. Raether, *Excitations of Plasmons and Interband Transitions by Electrons* (Spinger-Verlag, Berlin, 1980).

[40] J. Fink, Adv. Electron. Electron Phys. **75**, 121 (1989).

[41] W. Ho, R. F. Willis, and W. E. Plummer, Phys. Rev. Lett. **40**, 1463 (1978).

[42] J. J. M. Michiels, J. E. Inglesfield, C. J. Noble, V. M. Burke, and P. G. Burke, J. Phys.: Condens. Matter **9**, L543 (1997).

[43] F. Müller, P. Steiner, Th. Straub, D. Reinicke, S. Palm, R. de Masi, and S. Hüfner, Surf. Sci. **442**, 485 (1999).

[44] F. Müller, R. de Masi, P. Steiner, D. Reinicke, M. Stadtfeld, and S. Hüfner, Surf. Sci. **459**, 161 (2000).

[45] H. Hopster, Phys. Rev. B **42**, 2540 (1990).

[46] M. P. Seah and W. A. Dench, Surf. Interface Anal. **1**, 2 (1979).

[47] R. C. Felton, M. Prutton, J. A. D. Matthew, and W. Zinn, Surf. Sci. **79**, 117 (1979).

[48] Thomas Dodt, Ph.D. thesis, University of Düsseldorf, 1988.

[49] D. T. Pierce, R. J. Celotta, G.-C. Wang, W. N. Unertl, A. Galejs, C. E. Kuyatt, and S. R. Mielczarek, Rev. Sci. Instrum. **51**, 478 (1980).

[50] K. J. Fischer, U. Köbler, B. Stroka, K. Bickmann, and H. Wenzl, J. Cryst. Growth **128**, 846 (1993).

[51] E. B. Bas, U. Bäninger, and H. Mülethaler, Jpn. J. Appl. Phys., Suppl. **2**, 671 (1974).

[52] J. E. Rowe, M. Campagna, S. B. Christman, and E. Bucher, Phys. Rev. Lett. **36**, 148 (1976).

[53] V. T. Rajan and L. M. Falicov, Solid State Commun. **21**, 347 (1977).

[54] F. P. Netzer and J. A. D. Matthew, in *Handbook on the Physics and Chemistry of Rare Earth Metals* edited by K. A. Gschneidner, Jr., L. Eyring, and S. Hüfner (North-Holland, Amsterdam, 1987), Vol. 10, p. 547ff.

[55] A. Gorschlüter and H. Merz, Phys. Rev. B **49**, 17 293 (1994).